Unsteady Simulation of Burning Off Carbon Deposition in a Coke Oven

Uzu-Kuei Hsu, Keh-Chin Chang, Joo-Guan Hang

Abstract—Carbon Deposits are often occurred inside the industrial coke oven during coking process. Accumulation of carbon deposits may cause a big issue, which seriously influences the coking operation. The carbon is burning off by injecting fresh air through pipes into coke oven which is an efficient way practically operated in industries. The burning off carbon deposition in coke oven performed by Computational Fluid Dynamics (CFD) method has provided an evaluation of the feasibility study. A three dimensional, transient, turbulent reacting flow simulation has performed with three different injecting air flow rate and another kind of injecting configuration. The result shows that injection higher air flow rate would effectively reduce the carbon deposits. In the meantime, the opened charging holes would suck extra oxygen from atmosphere to participate in reactions. In term of coke oven operating limits, the wall temperatures are monitored to prevent over-heating of the adiabatic walls during burn-off process.

Keywords—Coke oven, burning off, carbon deposits, carbon combustion, CFD.

I. INTRODUCTION

IN an industrial coking process, coal is placed in a heated coke oven. Under the condition of high thermal energy and lack of oxygen, the pyrolysis process converted coal into coke while some of the hydrocarbons emerge as volatile matters. The hydrocarbons may undergo pyrolysis process on the heated wall surface and, then, forms carbon deposits on the wall. The mechanism of forming carbon deposits is a complex process [1]-[5] which has involved of gas-phases decomposition, dehydrogenation, gas-solid reactions, nucleation and growth on the surface. The growth rate of carbon deposits is affected by several factors, such as temperature, type of source gas, concentration of source gas, and the coal moisture content. The Coal Moisture Control (CMC) technology [6] has been introduced to dehydrate ordinary wet coal before get into coking process. The CMC process has improved the coking productivity and reduced heat consumption. On the other hand, [7] experimentally found that the CMC treated coal would produce 45% to 75% more carbon deposits in comparison with those in wet condition. Vrebs et al. [8] has studied the effects of coal moisture content on the formation of carbon deposits. They observed that the carbon deposition rate was decreased by

U. K. Hsu is with the Department of Aircraft Engineering, Air Force Institute of Technology, Koashiung 82063, Taiwan (corresponding author to provide phone: +886-7-6254168; e-mail: ukhsu@ms48.hinet.net).

K. C. Chang and J. G. Hang are with the Institute of Aeronautics and Astronautics, National Cheng Kung University, Tainan 701, Taiwan (e-mail: kcchang@mail.ncku.edu.tw, mikahang13@hotmail.com).

increasing the moisture content up to 8 % wt. For higher moisture content, the rate was increased dramatically. In Japan, [9] studied the injection of atomized water in the free spaces of coke oven during the coking process. They observed that the temperature in coke oven chamber was decreased because the evolved heat has been consumed by injecting water, as well as the carbon deposits were decreased. The growth and mechanisms of carbon deposits has been studied in order to understand and control the carbon deposits. There are several methods adopted to eliminate or remove the carbon deposits. One of the presently used methods is manual removal, but it requires a period of time to shut down the coke oven for removing process. Another method is to burn off carbon deposition by inducing air through inject pipe into coke oven from opened charging hole. The coke oven is required to be emptied during the burn-off process. This method operates conveniently and decreases the production lost in term of operation time. Furthermore, the burn-off method is practically operated in industries at present.

To burn off the carbon deposition in the coke oven, [10] experimentally found that the composition of carbon deposits depends upon their locations in the coke oven. According to their study, the carbon deposits contain low ash mixture of pyrolytic carbon and char which can be considered as a specific case of solid carbon combustion in air. Furthermore, [11] studied the reaction kinetics of carbon deposit with air. They showed that the combustion rate of carbon deposits with air has improved efficiently when temperature above 1400 K. The burning of carbon is classified as one-firm model and two-firm model [12]. In the assumptions of one-firm model, only heterogeneous reactions occur on carbon surface. Thus, the surface bears the highest temperature. On the other hand, the two-firm model has considered homogeneous reaction of CO with O_2 which reacts into CO_2. On the carbon surface, CO is mostly produced due to the lack of O_2. With participation of the homogeneous reaction, CO on wall burns in a thin flame sheet in boundary layer. In the meantime, most of O_2 could not reach the carbon surface as the homogeneous reaction is a fast reaction. The produced CO_2 then diffuses inward and reacts with carbon surface, forming CO again. The two-firm model illustrates more realistic carbon combustion phenomena in comparison with one-firm model.

A simplified model of carbon combustion in a stagnant boundary layer has been performed numerically by [13]. The molecule diffusion is the only transport of the gas phase species in boundary layer with neglecting the buoyancy effect. They numerically studied feasible regions for one-dimensional steady state carbon combustion under mass and energy

conservation. The combustion behavior of carbon surface has been performed theoretically by [14]. In the temperature range of 1200 to 2000 K, the combustion rate is strongly influenced by the homogeneous reaction which could not negligible or assumed to be infinitely fast reaction. Yi et al. [15] simulated quiescent carbon combustion in air. Simulations with several sizes of carbon particles and variety of ambient parameters, such as air temperatures and ambient velocity, have been studied respectively. Three of the carbon combustion regimes have been performed, namely diffusion-controlled, kinetic-diffusion-controlled, and kinetic-controlled regimes. The carbon burn-off time of different combustion regimes has also been shown in the study. The influence of heterogeneous kinetics of carbon consumption has been studied numerically by [16]. By comparing the carbon consumption rate, the result showed that the selection of chemical kinetic data could cause 300-400% discrepancy of carbon mass flux. A steady state simulation of burning off carbon deposition in coke oven has presented by [10]. They assumed that the carbon deposits accumulated on the charging holes and top roof surfaces. The modelling of carbon combustion only considered the heterogeneous reaction on carbon surface, and produced carbon dioxide instantly. The result showed that carbon dioxide to be accumulated in the closed charging holes which may not eliminate the carbon deposits.

The purpose of this paper is to provide an evaluation of the feasibility study on burning off the carbon deposition in coke oven numerically. The Computational Fluid Dynamics (CFD) simulation provides a prediction and analysis of carbon deposition burn-off problems. In the present study, a three-dimensional coke oven in empty state has been simulated numerically. Four different types of injecting flow configurations have been performed, to investigate the feasibility and efficiency of burning off carbon deposits.

II. PHYSICAL MODELLING

A. Problem Description

A typical structure of industrial coke oven consists of four goosenecks as charging holes, a chimney, and two oven doors along with side walls. A combustion chamber is placed between coke ovens side by side, which is arranged to provide heat by sharing the side wall. The produced coke is then guided by the moving pusher door to leave coke oven from door nearby the chimney and is transported to the next process. After that, the pusher door returns to its origin and coke oven stays closed. The burn-off method operates when coke oven is empty before it gets charged for the next coking process again. Meanwhile, the side wall remains heated. In the present study, the coke oven simulation assumes the side wall is heated symmetrically, the top and the bottom wall are isolated, and the two oven doors are stationary. The carbon deposits are mainly accumulated beneath top roof, charging holes, and two-fifths of the side wall. The schematic figure of contemporary coke oven simulation is shown in Fig. 1. According to Fig. 1, the computational domain reduces by half as it is symmetry along y-direction and the symmetry plane is located on y=0.

The carbon chemical kinetic reactions in combustion and a comprehensive physical modelling involved turbulent transport, species transport, and radiation of the fluid flow will be described in the following sections.
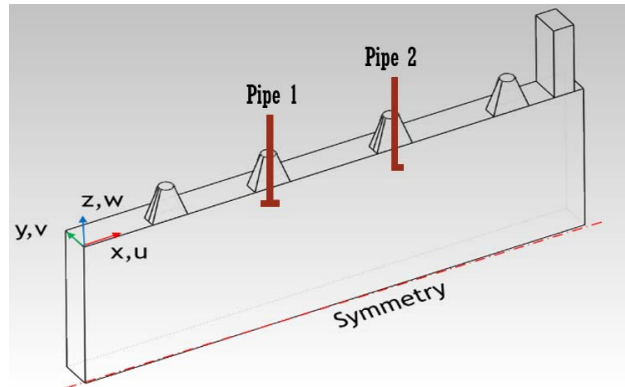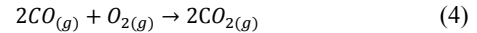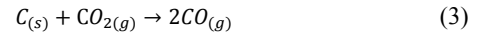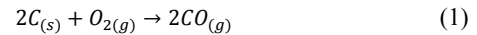

Fig. 1 The schematic of simulation geometry

B. Carbon Combustion Model

At present, the carbon combustion in air involves O_2, CO, CO_2 and N_2 gas species. The chemical reaction formulas are written as,

$$2C_{(s)} + O_{2(g)} \rightarrow 2CO_{(g)} \qquad (1)$$
$$C_{(s)} + O_{2(g)} \rightarrow CO_{2(g)} \qquad (2)$$
$$C_{(s)} + CO_{2(g)} \rightarrow 2CO_{(g)} \qquad (3)$$
$$2CO_{(g)} + O_{2(g)} \rightarrow 2CO_{2(g)} \qquad (4)$$

Reactions (1), (2), and (3) are the heterogeneous reactions on the carbon surface. Reactions (1) and (2) are the exothermic reactions which oxidize carbon into carbon monoxide and carbon dioxide, respectively. Reaction (3) is the endothermic reaction of carbon dioxide into carbon monoxide. Reaction (4) is the homogeneous reaction of carbon monoxide and oxygen which reacts exothermically into carbon dioxide. In summary, the chemical reaction rates [15], [17] can be expressed in Arrhenius form as,

$$R_1 = -A_1 \exp\left(-\frac{E_1}{RT}\right) \rho_s Y_{O_2} \ (kg/m^2s) \qquad (5)$$
$$R_2 = -A_2 \exp\left(-\frac{E_2}{RT}\right) \rho_s Y_{O_2} \ (kg/m^2s) \qquad (6)$$
$$R_3 = -A_3 \exp\left(-\frac{E_3}{RT}\right) \rho_s Y_{CO_2} \ (kg/m^2s) \qquad (7)$$
$$R_4 = -A_4 \exp\left(-\frac{E_4}{RT}\right) \rho^2 Y_{CO} Y_{O_2} \ (kg/m^3s) \qquad (8)$$

where the heterogeneous reaction rates are considered to be first order kinetic rate proportional to the concentration of gas reactant on carbon surface. For gas phase reaction, the reaction rate is a second order reaction of CO and O_2 concentrations. All the reaction kinetic coefficient constants, as well as the heat of reactions, are summarized in Table I.

The homogeneous reaction of CO and O_2 is a fast reaction. The chemical reaction rate is relatively faster in comparison to the turbulent mixing. Thus, the interaction of turbulent eddy with chemical reaction rate is considered as an important factor

to influence combustion phenomena. The Eddy-Dissipation Model has been proposed by [18].

REACTION (i)	A_i	E_i/R (K)	$\Delta H_i (kJ/mol)$
1	1813	1.31×10^4	-110.53
2	1225	1.2×10^4	-393.52
3	7351	1.66×10^4	172.46
4	7×10^4	8×10^3	-282.99

The rate of reaction is determined by turbulent eddy mixing of the fuel over oxygen or oxygen over the fuel. In premixed turbulent combustions, the reaction rate is product-dependent, as turbulent eddy mixes hot product with cold reactants, providing heat to react. The Eddy-Dissipation Model governs rate of reaction as (9) and (10). The rate of production of species i due to reaction r, $R_{i,r}$ is expressed as,

$$R_{i,r} = v'_{i,r} MW_i A \rho \left(\frac{\epsilon}{k}\right) \min_{\mathcal{R}} \left(\frac{Y_\mathcal{R}}{v'_{\mathcal{R},r} MW_\mathcal{R}}\right) \qquad (9)$$

$$R_{i,r} = v'_{i,r} MW_i AB \rho \left(\frac{\epsilon}{k}\right) \left(\frac{\sum_P Y_P}{\sum_P v''_{P,r} MW_P}\right) \qquad (10)$$

where $Y_\mathcal{R}$ is the mass fraction of particular reactant, $\mathcal{R}$; Y_P is the mass fraction of any product species, P; $A = 4.0$ is an empirical constant; $B = 0.5$ is an empirical constant.

The rate of reaction is governed by the eddy mixing time scale, (k/ϵ). In simulation, the Eddy-Dissipation reaction rates and the Arrhenius reaction rate are calculated. With comparison, the minimum is selected as reaction rate which is determined as diffusion-controlled if the Eddy-Dissipation reaction rate is taken, the reaction is said to be mixing-limited. Alternatively, the reaction is kinetic-controlled in the other way.

At the same time, the heterogeneous reaction rates represents the reduction of carbon deposits on surface. The reduction length is defined as (11), which is the integration of reduction rate through time.

$$Reduction\ Rate: \quad \dot{L}_R = R_C \times MW_C \times \frac{1}{\rho_C} \qquad (11)$$

where $\dot{L}_R (m/s)$ is the reduction rate of carbon deposits, $R_C = \sum_i R_i$ is the summation of heterogeneous reaction rates, $MW_C = 12.011\ kg/kmol$ is molecular weight of carbon, $\rho_C = 2267\ kg/m^3$ is density of carbon.

C. Theoretical Model

A set of conservation equations and transport equations need to be solved numerically in turbulent combustion problem, which included conservation of mass, species, momentum, energy, and turbulent transport equations, and equation of state. Low Reynolds number turbulent model has been used in the numerical approach, as the reactions involved on the surface influence simultaneously in boundary layer. Realizable k-ε model proposed by [19] has been introduced to perform a better recover in turbulent viscosity at viscous sublayer region.

1) Continuity Equation:

$$\frac{\partial \rho}{\partial t} + \frac{\partial (\rho u_i)}{\partial x_i} = 0 \qquad (12)$$

2) Momentum Equation:

$$\frac{\partial}{\partial t}(\rho u_i) + \frac{\partial}{\partial x_j}(\rho u_i u_j) = -\frac{\partial P}{\partial x_i} + \rho \bar{g}_i + \frac{\partial}{\partial x_j}\left[(\mu + \mu_t)\left(\frac{\partial u_i}{\partial x_j} + \frac{\partial u_j}{\partial x_i} - \frac{2}{3}\delta_{ij}\frac{\partial u_i}{\partial x_j}\right) - \frac{2}{3}\delta_{ij}k\right] \qquad (13)$$

where, the eddy viscosity is $\mu_t = \rho C_\mu \frac{k^2}{\epsilon}$. The C_μ is a function of mean strain rate, suggested by [19].

3) Turbulent Kinetic Energy Transport Equation:

$$\frac{\partial}{\partial t}(\rho k) + \frac{\partial}{\partial x_j}(\rho k u_j) = \frac{\partial}{\partial x_j}\left[\left(\mu + \frac{\mu_t}{\sigma_k}\right)\frac{\partial k}{\partial x_j}\right] + G_k + G_b - \rho \epsilon \qquad (14)$$

4) Turbulent Dissipation Energy Transport Equation:

$$\frac{\partial}{\partial t}(\rho \epsilon) + \frac{\partial}{\partial x_j}(\rho \epsilon u_j) = \frac{\partial}{\partial x_j}\left[\left(\mu + \frac{\mu_t}{\sigma_\epsilon}\right)\frac{\partial \epsilon}{\partial x_j}\right] + \rho C_1 S\epsilon - \rho C_2 \frac{\epsilon^2}{k+\sqrt{v\epsilon}} + C_{1\epsilon}\frac{\epsilon}{k}C_{3\epsilon}G_b \qquad (15)$$

where $C_1 = \max\left\{0.43, \frac{\eta}{\eta+5}\right\}$, $C_{3\epsilon} = tanh\left|\frac{v}{u}\right|$, $\eta = S\frac{k}{\epsilon}$, $S = \sqrt{2S_{ij}S_{ij}}$, $S_{ij} = \frac{1}{2}\left(\frac{\partial u_j}{\partial x_i} + \frac{\partial u_i}{\partial x_j}\right)$, Turbulent Production: $G_k = -\rho\overline{u_i'u_j'}\frac{\partial u_j}{\partial x_i} = \mu_t S^2$, Effect of Buoyancy: $G_b = \beta g_i \frac{\mu_t}{Pr_t}\frac{\partial T}{\partial x_i}$

The turbulent model coefficients are summarized in Table II.

$C_{1\epsilon}$	1.44	σ_ϵ	1.2
C_2	1.9	Pr_t	0.85
σ_k	1	Sc_t	0.7

5) Species mass Fraction Equation:

$$\frac{\partial}{\partial t}(\rho Y_i) + \frac{\partial}{\partial x_j}(\rho u_j Y_i) = \frac{\partial}{\partial x_j}\left[\left(\rho D_{i,m} + \frac{\mu_t}{Sc_t}\right)\frac{\partial Y_i}{\partial x_j} + \frac{D_{T,i}}{T}\frac{\partial T}{\partial x_j}\right] + \mathcal{R}_i \quad (16)$$

where, $i = O_2, CO, CO_2$ the first term in right hand side of equation is the diffusion flux term of species i which has included mass diffusivity, turbulent eddy diffusion and Soret Effect. The thermal diffusivity coefficient introduced by [20], showed in (17):

$$D_{T,i} = -2.59 \times 10^{-7} \times T^{0.659} \times \left[\frac{M_{w,i}^{0.511}X_i}{\sum_{i=1}^N M_{w,i}^{0.511}X_i} - Y_i\right]\left[\frac{\sum_{i=1}^N M_{w,i}^{0.511}X_i}{\sum_{i=1}^N M_{w,i}^{0.489}X_i}\right] (17)$$

The second term of right hand side is the mass of production by (4). The mass fraction of N_2 is calculated by the conservation of mass fraction, $Y_{N_2} = 1 - Y_{CO} - Y_{CO_2} - Y_{O_2}$.

6) Energy Equation:

The energy equation expressed in form of sensible enthalpy.

$$\frac{\partial}{\partial t}(\rho h) + \frac{\partial}{\partial x_j}(\rho h u_j) = \frac{\partial}{\partial x_j}\left(\frac{\lambda_{eff}}{C_p}\frac{\partial h}{\partial x_j} - \sum_k h_k \bar{J}_k\right) + \frac{Dp}{Dt} + S_R \quad (18)$$

where, $h = \sum_k h_k Y_k$; $h_k = \int_{T_{ref}}^T C_{p,k}(T)dT$; $C_p(T) = \sum_k Y_k C_{p,k}(T)$;

$\bar{J}_k = -\left(\rho D_{m,k} + \frac{\mu_t}{Sc_t}\right)\frac{\partial Y_k}{\partial x_j} - \frac{D_{T,i}}{T}\frac{\partial T}{\partial x_j}$ is the mass flux transport term; $\lambda_{\text{eff}} = \lambda + \frac{C_p\mu_t}{\text{Pr}_t}$;and S_R included heat of radiation and (4).

$$S_{Reaction} = -h_4^o R_4 \qquad (19)$$

$$S_{Radiation} = \alpha G - 4\alpha n^2 \sigma T^4 \qquad (20)$$

where G is incident radiation flux. The P-1 Radiation Model [21] has been choose to solve the reacting flow incident radiation transport equation as (21). The Weighted-Sum-of-Gray Gases Model (WSGGM) has applied for CO_2 to compute gas phase emissivity coefficient [22], as well as absorption coefficient showed in (22) and (23):

$$\frac{\partial}{\partial x_i}\left(\frac{1}{3\alpha}\frac{\partial G}{\partial x_i}\right) - \alpha G + 4\alpha n^2 \sigma T^4 = 0 \qquad (21)$$

$$\varepsilon = \sum_{i=0}^{3} a_{\varepsilon,i}(\text{T})[1 - e^{-\kappa_i ps}] \qquad (22)$$

$$\alpha = -\frac{\ln(1-\varepsilon)}{s} \qquad (23)$$

7) Equation of State:

$$P = \rho_g R T_g \qquad (24)$$

The chemical species mixture such as density, specific heat, thermal conductivity, and viscosity is derived by Ideal gas mixing-law [20].
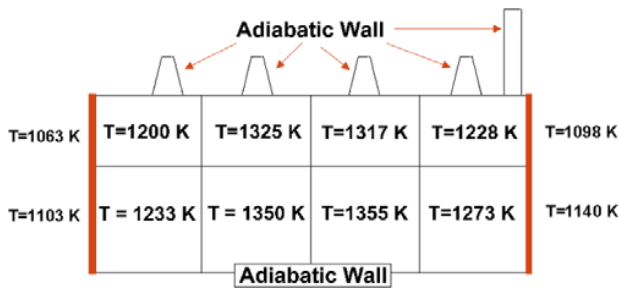
Fig. 2 The temperature distributions of coke oven

D. Boundary Conditions

The boundary conditions of coke oven are considered as a wall which is of no slip condition along with the gradient of species concentration equals to zero. The wall temperature distributions are practically measured from a realistic coke-oven side wall by infrared thermometer, as shown in Fig. 2. Besides, the bottom wall, top roof, charging holes, and chimney are assumed to be under adiabatic condition. Furthermore, the charging holes, top roof and two-fifths of the side wall are treated as with carbon depositions where the heterogeneous reactions happen. The species mass fraction requires the mass conservation on surface corresponding to the production or destruction rate written as,

$$\rho_s D_{m,i}\left(\frac{dY_i}{dy}\right)_{wall} = -R_i \qquad (25)$$

where i corresponding to species O_2, CO, CO_2. Similarly, the energy must be balanced due to heat of reactions on carbon surfaces. Thus, the energy conserve on the boundary as,

$$-\lambda\left(\frac{dT}{dy}\right)_{wall} = \sum_k \Delta H_k R_k + q_{r,w} \qquad (26)$$

where $q_{r,w}$ is computed from the P-1 Radiation Model boundary condition as,

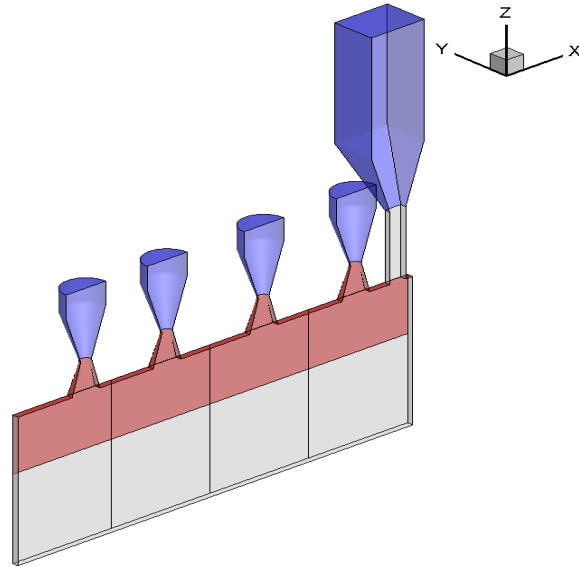$$q_{r,w} = -\frac{\varepsilon_w}{2(2-\varepsilon_w)}(4n^2\sigma T_w^4 - G_w) \qquad (27)$$

Fig. 3 The schematic of computational domain

On the other hand, the flow inlets injecting fresh air into the coke oven are set as prospective mass flow rate with temperature of 300K containing 21% of oxygen ($Y_{O_2} = 0.233$). During the burn-off operation, the tops of charging holes are opened to place the injecting pipes into coke oven. The boundary conditions for the opened charging holes are hardly measured from realistic situation and impossibly held in specific conditions with transient problem. The interaction between the exhaust gas mixture and atmospheric nature air is an important factor affecting coke oven simulation. Thus, the extension of computational domain is required to artificially construct an environment outside of the coke oven. The boundary conditions for the extended computational domain is assumed to be at atmospheric pressure (1 atm), and the gradient of temperature and species concentration are equal to zero. Fig. 3 shows a complete computational domain covered in the present study, where the red parts are where carbon deposits take place, and the blue parts represent extended computational subdomains.

III. NUMERICAL ANALYSIS

A. Numerical Method

The commercial simulation software ANSYS-Fluent v.13.0 has been employed in the present study which had been

developed comprehensively and used widely over the last decade for computational fluid dynamics (CFD). In the present study, the SIMPLEC algorithm is employed. The advection terms in the governing equations are discretized by Second-Order Upwind Scheme. Furthermore, a second-order accuracy's Central-Differencing Scheme is used to discretize the diffusion terms. The Body-Force-Weighted Scheme is selected for pressure discretization scheme as the combustion occurrence may enhance large variation of density, thus buoyancy force is induced. The amount of computational nodes is approximately 5.7×10^6. The Intel Xeon E5645 dual processors (with 32GB RAM) is employed as the computing instrument for the study.

B. Initial Conditions Simulation

Before the burn-off process being simulated (t<0), a reasonable initial condition has to be performed in a way close to the real situation as follows. All of the charging holes except the chimney are initially closed which are isolated from atmospheric air. The carbon combustion starts with the existent air in the coke oven. In the meantime, the chimney is the only route connecting the suction of fresh air and the coke oven's exhaust gas. The initial condition is simulated under steady state condition.

C. Transient Simulation

With the initial condition obtained as mentioned above, the transient simulation is executed. At the beginning of transient simulation (t=0), four of the charging holes is opened instantaneously. In the meantime, the fresh air is blowing into coke oven through a pipe which is pull down from the assigned charging holes (see Fig. 4). The configuration of impinging jet is designed with certain amount of mass flow rate. Besides, to prevent the numerical divergence due to the highly non-linear sources term, such as reaction rate. The time step is fixed as Δt=0.0005 s which is less than the chemical time scale. Besides, the unsteady terms are discretized by first-order implicit scheme. Each of the time step has to be converged to advance the next time step iteratively.
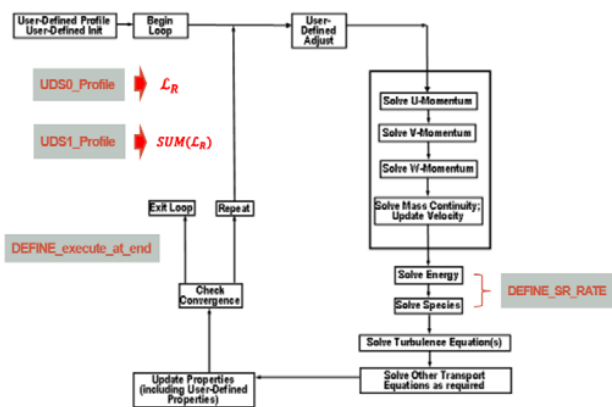

Fig. 4 The UDFs hooking function

IV. RESULTS AND DISCUSSIONS

A. Initial Conditions of Coke Oven

The coke oven is in empty condition all along the burn-off process. All of the charging holes are closed initially. In the meantime, the only interaction between the interior gases and atmospheric fresh air is through the route of the chimney. The initial conditions are simulated as a steady-state solution of coke oven. A part of the coke oven is considered to be accumulated with a certain thickness of carbon deposits on the surface, which is shown in Fig. 5. The carbon thickness is linearly grown from three-fifths of the height of side wall, as well as the charging holes and beneath roof are deposited with the thickness of 10 mm.

In this situation, the coke oven is heated from the side wall constantly, as shown in Fig. 6. Due to insufficient oxygen, the carbon deposits produce great amount of CO which is resided in the coke oven.
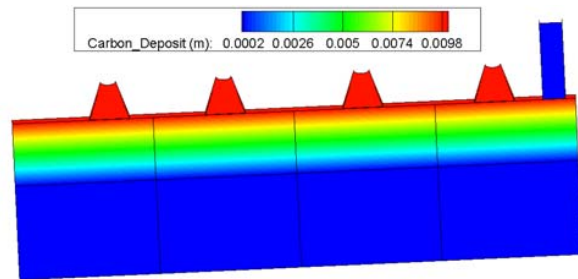

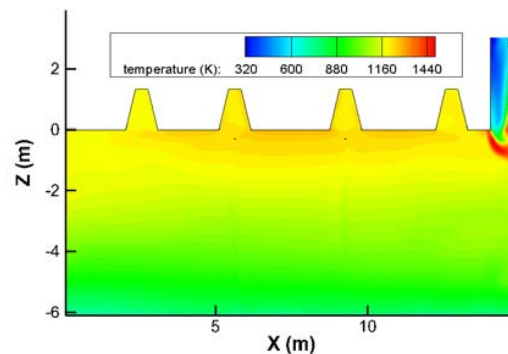Fig. 5 The distribution of carbon deposits initially

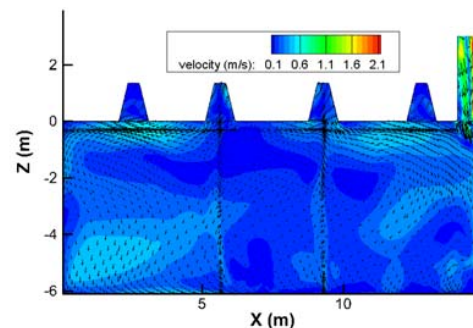
Fig. 6 The initially distributed temperature

Fig. 7 The initial velocity distribution

Furthermore, the natural convection leads lighter gas mixture move toward exterior atmosphere. Then, fresh air simultaneously convected into coke oven due to mass conservation. The velocity distribution is shown in Fig. 7 that fresh air is convected from one side while the interior gas mixture flow out from another side of chimney. The fresh air reacts with the accumulated CO in the coke oven and, then, produces CO_2. Thus, the highest temperature occurred below the chimney where the exothermic reaction takes place. In addition, the burning of carbon happens on the surface near to the highest temperature regions. With the descriptions above, the initial conditions are more close to the practical situation of coke oven. The burning of carbon is hardly occurs at insufficient oxygen condition.

B. Cases Study of Coke Oven

The initial conditions as above mentioned are employed for the following cases study. At the beginning of transient simulation (t = 0), four of the charging holes are set open to the ambient environment. This is because the heat of reaction would be accumulated inside the charging holes and the temperatures would be abnormally increased due to the adiabatic boundary conditions in the previous simulations when the charging holes are closed. In the meantime, Pipe 1 has been put into the coke oven through the Inlet 2 and Pipe 2 has put through the Inlet 3. Both placed at the height of $z = -0.3\ m$. The pipe sizes are 3/4'' diameter. The Pipe 1 blows toward front (i.e., toward chimney direction) and rear (i.e., toward pushing door direction) direction, while horizontal to x-axis. While the Pipe 2 only blows toward the front direction. There are three cases with different volumetric flow rates and another case with different configurations are studied.

1. Case 1: 5000 LPM fresh air blows from Pipe 1.
2. Case 2: 10000 LPM fresh air blows from Pipe 1.
3. Case 3: 20000 LPM fresh air blows from Pipe 1.
4. Case 4: 5000 LPM fresh air blows from Pipe 1 and 2500 LPM from Pipe 2.

Plane A-A which is the cross-section of the pipe in Fig. 8 is presented to analyze the effect of the different blowing flow rates on the performance of burning-off of carbon deposits. At time of 1.3 s, the velocity distributions of Case 1 and Case 2 at the Plane A-A are shown in Fig. 9 where the upper half is the Case 1's result, while the lower half is the Case 2's result, and the symmetry line at y = 0. The temperature distribution of the Case 1 is higher than that of the Case 2 due to larger air flow rate bringing in more nitrogen which do not contribute in the reactions and absorb some heat of reactions to increase the temperature of nitrogen species. Due to the higher velocity, the oxygen is propagated more far as well. The distribution of oxygen (Fig. 10) shows that it is unable to reach the carbon surface as the reaction took place in gas phases and formed carbon dioxide, as the distributions of carbon dioxide and carbon monoxide showed in Figs. 11 and 12, respectively. The produced carbon dioxide is able to transport to the surface of carbon deposits, reducing the carbon deposit thickness by the reaction of carbon and CO_2. The comparison among the present cases shows that the larger air flow rate transports CO_2 more far

and performs larger effective area. In comparison to Case 3, the physical phenomena are similarly happened as the previous discussion for higher air flow rate. The thermal diffusivities are very small in comparison to the molecular diffusivities, as shown in Figs. 13 and 14. Thus, the thermal diffusivities are negligible in present work.
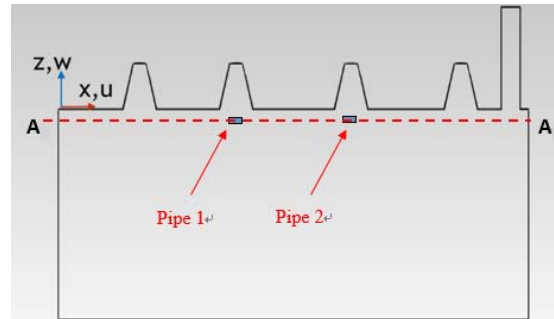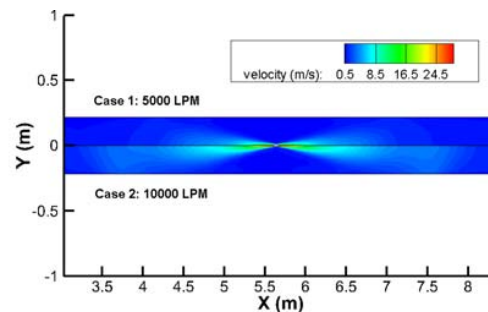

Fig. 8 The Plane A-A: Cross section of the pipes

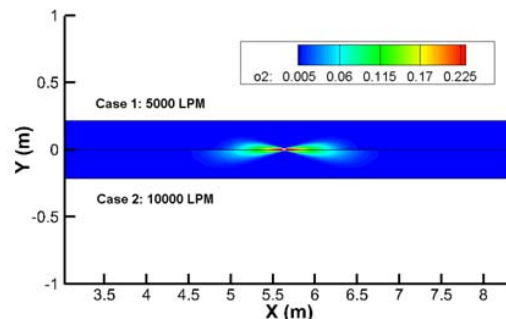Fig. 9 The velocity distributions of Plane A-A

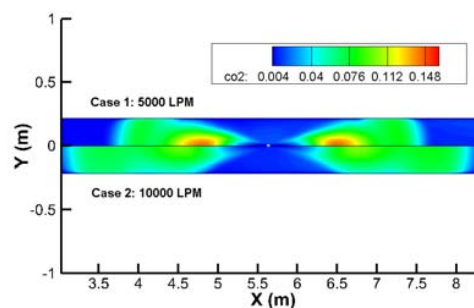Fig. 10 The O_2 mass fraction distributions of Plane A-A

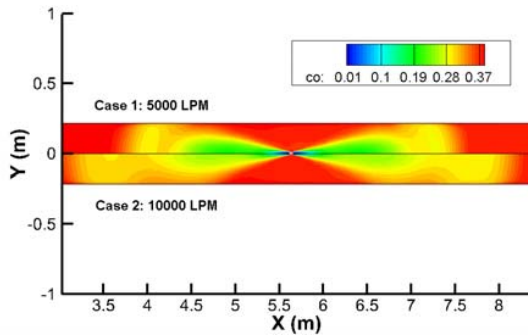Fig. 11 The CO_2 mass fraction distributions of Plane A-A

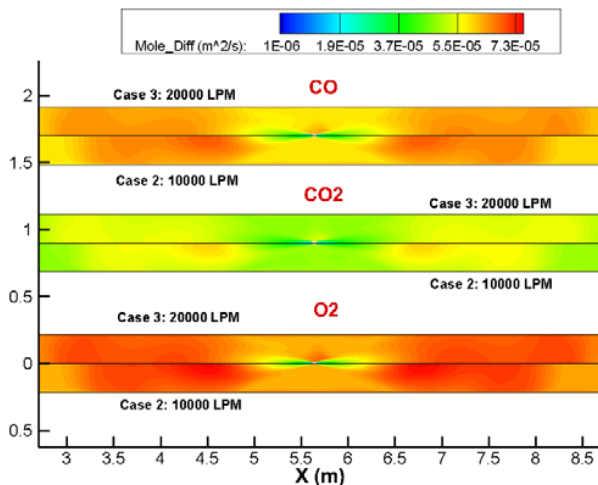Fig. 12 The CO mass fraction distributions of Plane A-A

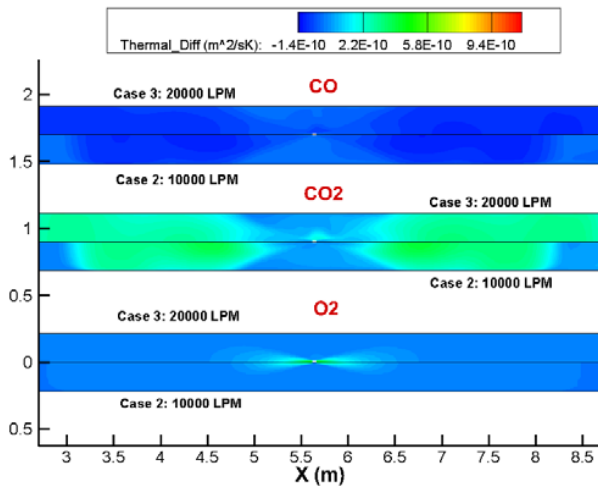Fig. 13 The molecular diffusivities distributions of Plane A-A

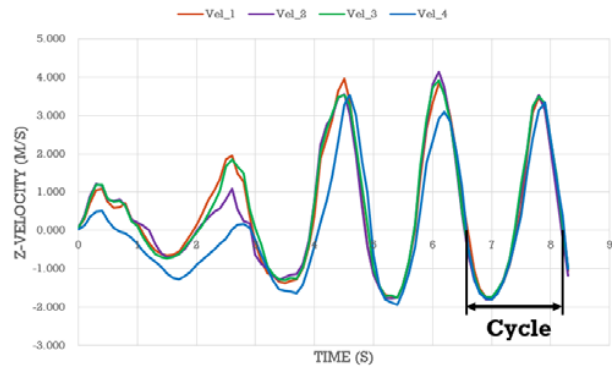Fig. 14 The thermal diffusivities distributions of Plane A-A

Fig. 15 The z-velocity of Inlets versus time distribution

C. Analysis of Quasi-Periodic Motion

As above mentioned, the sucking of oxygen "balloons" occurred regularly when the charging holes were opened. The quasi-periodic motion of air flow in and out from the charging holes act like a breathing process. The quasi-periodic motion is inspected by its z-directional velocity distribution, as shown in Fig. 15. There are four velocity lines (as Vel_1, Vel_2, Vel_3 and Vel_4) in which the Vel_1 represents the z-directional velocity of Inlet 1 with respect to time, and so on. Four of the Inlets possess a transient flow motions when they were opened initially. After 4 seconds, the oscillations of z-directional velocities become obvious. As time elapsed, four of the velocity distributions get closer to each other, and become nearly synchronized. Thus, the complete cycle of the flow motion is defined as quasi-periodic motion of the coke oven. In addition, five of the different situations (as shown in Fig. 16) of the quasi-periodic motion are analyzed by their own pressure and velocity distributions in the coke oven. At Point 1, the air begins to flow in and the pressure distribution is showed in Fig. 17 which indicates the pressure in the coke oven is slightly less than atmospheric pressure.

Corresponding to each periodic motion, a vortex has generated by the oxygen "balloon" beneath the top wall. At the time 7.8 s, one of the vortexes below the Inlet 3 is showed in Fig. 18 that it is at the middle (located at $z = -1.5\,\mathrm{m}, x = 9.5\,\mathrm{m}, y = 0\,\mathrm{m}$) of a square meters area. The frequency of periodic motion at Inlet 3 with the location of $z = -1.5\,\mathrm{m}, x = 9.5\,\mathrm{m}$ and $y = 0\,\mathrm{m}$ is plotted with respect to time. The z-directional velocities shown in Fig. 19 reveals that the frequency of vortex beneath the top wall is about half cycle delayed in comparison to the frequency of Inlet 3. In the meantime, the temperature distributions at 4 different locations (surrounding the middle point, as $z = -1\,\mathrm{m}, x = 10\,\mathrm{m}, y = 0\,\mathrm{m}$; $z = -2\,\mathrm{m}, x = 10\,\mathrm{m}, y = 0\,\mathrm{m}$; $z = -1\,\mathrm{m}, x = 9\,\mathrm{m}, y = 0\,\mathrm{m}$; $z = -2\,\mathrm{m}, x = 9\,\mathrm{m}, y = 0\,\mathrm{m}$) are plotted with respect to time, as shown in Fig. 20. The temperature distributions showed that the averaged temperature in the coke oven is about 1200 K. The raising of temperatures as the oxygen "balloon" reacted and released heat. The period of the temperature dropped below 1000 K at the location of $z = -2\,\mathrm{m}, x = 10\,\mathrm{m}$ and $y = 0\,\mathrm{m}$ are observed. It explains that the vortex is moving toward the chimneys direction due to natural ventilation effect.
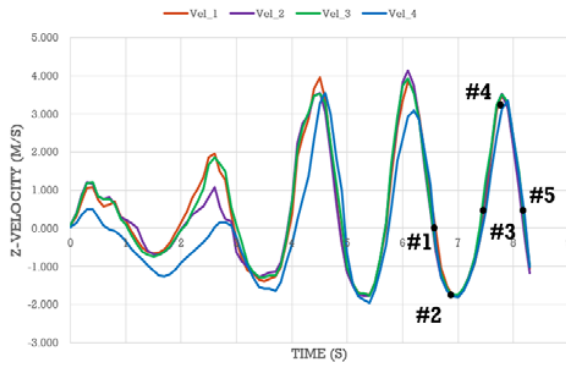
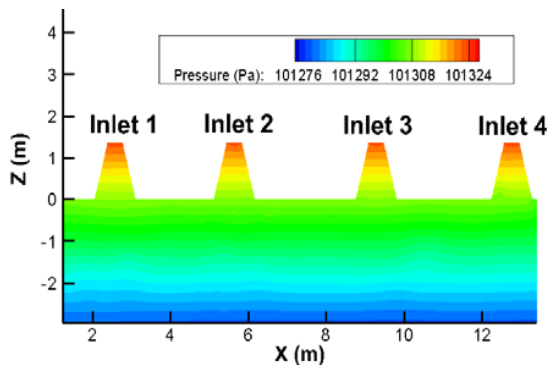Fig. 16 The analysis of the quasi-periodic motion at different positions
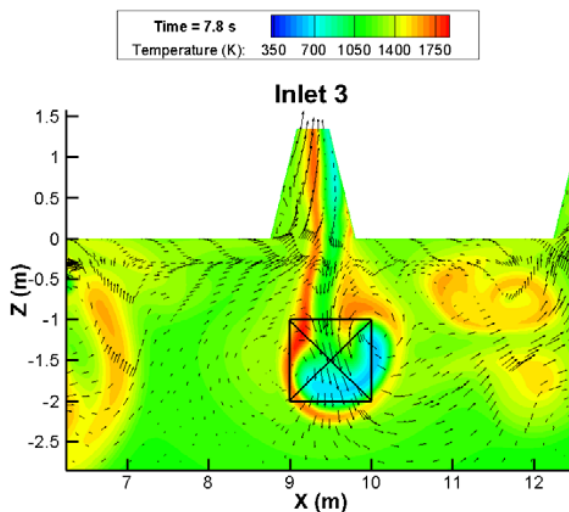

Fig. 17 The pressure distribution of Point 1

Fig. 18 The vortex beneath the Inlet 3 at time of 7.8 s

D. Prediction of Carbon Reductions

The quasi-periodic behavior of flow motion has been discussed in the previous section, like a breathing process. The phenomena of quasi-periodic motion are occurred due to the interaction between chemical reaction and natural ventilation. These phenomena continuously happen once the carbon deposits are able to react with carbon dioxide or oxygen, and, then, produce carbon monoxide in the coke oven. With the time elapsed, the influence of the initial conditions become less significant and the flow motion can gradually reach a quasi-periodic state. The complete cycle of quasi-periodic solution then provides a basis to predict the reduced thickness of carbon deposits. The Case 2's burn-off process is chosen to estimate the carbon reduction thickness on 60-minute operation time. The estimated reduction thickness of carbon deposits is shown in Fig. 21 that the burn-off process is able to reduce up to 1.8 mm carbon thickness.
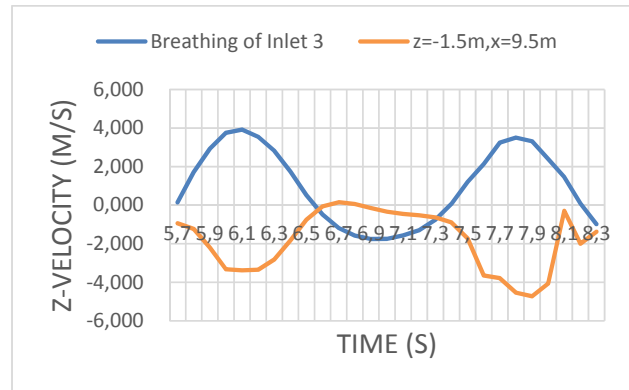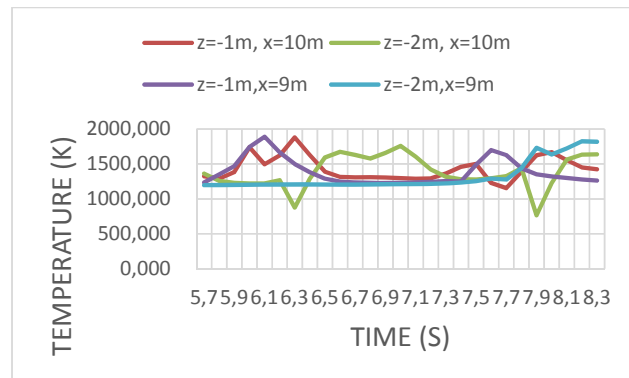

Fig. 19 Evaluation of z-directional velocity at Inlet 3 and vortex beneath (x=9.5 m,y=0 m and z=-1.5 m) versus time

Fig. 20 Evaluation of temperature distributions at 4 different locations versus time

The designed Pipe 1 with 10000 LPM air flow rate (Case 2) could remove about 1 mm carbon thickness on the side wall. The distribution of remaining percentages of carbon deposits is shown in Fig. 22 that the blowing air (Case 2) has removed about 10 % carbon deposits toward the front direction on side wall; while on the top wall (Fig. 23), the efficiency is slightly lower than side wall, about 5 % carbon reduction. However, the quasi-periodic motion has provided additional air into coke oven which contributed quite a lot in the process of removing carbon deposits. It has removed 20 to 30 % carbon deposits on the side wall, as shown in Fig. 22.
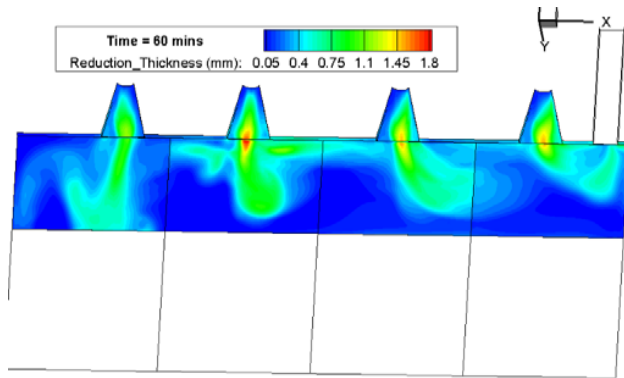
Fig. 21 The estimated reduction thickness of carbon deposits with 60-minute operation time
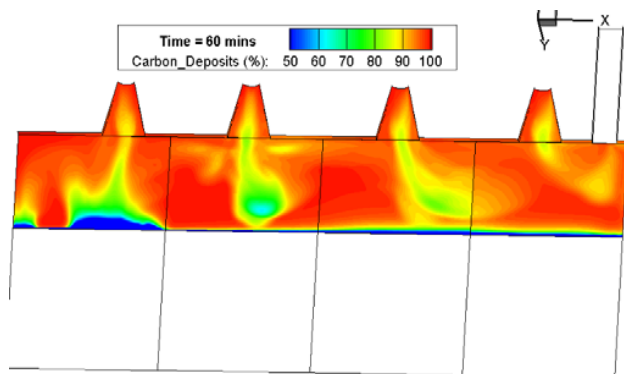

Fig. 22 The remaining percentages of carbon deposits with 60-minute operation time
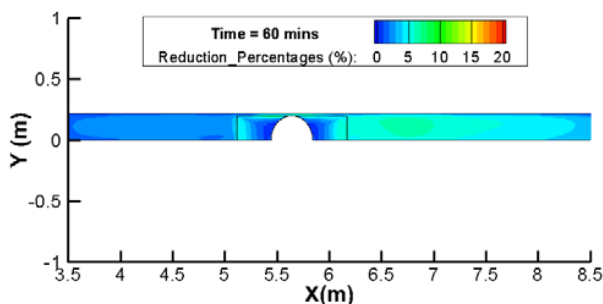

Fig. 23 The percentages of carbon reduction on top wall

V. CONCLUSIONS

The simulation results showed that the injections of air in the coke oven are feasible to remove carbon deposits by burn off process. With a designed configuration of injecting flows, the larger airflow rate would cause more effective reduction of carbon deposits. In the meantime, the charging holes were opened during the burn-off process. It has been observed that a quasi-periodic flow motion take place in the coke oven which is a physicochemical phenomenon caused by natural ventilation and combustion chemistry interaction. With the quasi-periodic solutions, it can provide a way to assess carbon reduction thickness. In the meantime, the opened charging holes can provide additional fresh air to burn-off process.

A complete numerical simulation requires plenty of computational time. However, the results presented here have taken three months of computational time. The number of computational nodes of the coke oven is as huge as about 5×10^7. With the involving of chemical reactions, the numerical time step has to be small enough to capture the physical phenomena, which increases the difficulty to solve the complex, non-linear, coupled governing equations.

With the lack of a true boundary conditions in coke oven, the current results are simulated by assuming that the neighboring combustion chambers are able to provide heat and control the coke oven in a stage of constant temperatures boundary conditions. It may be over-predicted the temperature of gases mixture and carbon reduction rates. For more precious solutions, the neighboring combustion chambers have to be taken into account in the modeling to perform a variable wall boundary conditions in the coke oven. It would require more computational nodes and complicated coupling between combustion chamber and coke oven chamber.

REFERENCES

[1] J. Patrick, R. Barranco, "Carbon Deposits: Formation, Nature, and Characterisation", *COMA/CRF Meeting*, United Kingdom, 2006.
[2] V. Krebs, F. Mareche, G. Furdin, D. Dumay, "Contribution to the Study of Carbon Deposition in Coke Ovens", *Fuel*, Vol. 73, No. 12, 1994, pp. 1904-1910.
[3] Z.J. Hu, K.J. Huttinger, "Mechanisms of Carbon Deposition-a Kinetic Approach", *Carbon*, Vol. 40, No. 4, 2002, pp. 624-628.
[4] K. Norinaga, K.J. Huttinger, "Kinetics of Surface Reactions in Carbon Deposition from Light Hydrocarbons", *Carbon*, Vol. 41, No. 8, 2003, pp. 1509-1514.
[5] Y. Z. Fang, P. Huang, Z. Zhang, Y.P. Cao, M.L. Jin, "Analysis on the Growth Mechanism of Carbon Deposits in Coke Oven", *Clean Coal Technology*, Vol. 17, No. 5, 2011, pp. 36-39. (In Chinese)
[6] Z. Z. Wang, Z. F. Zhan, W. D. Wang, W. D. Zhang, X. Q. Zhang, H. S. Wang, "Analysis and Research on Coal Moisture Control Technology", *Applied Energy Technology*, No. 3, 2014, pp. 5-9. (In Chinese)
[7] A. Furusawa, T. Nakagawa, Y. Maeno, I. Komaki, "Influence of Coal Moisture Control on Carbon Deposition in the Coke Oven Chamber", *ISIJ*, Vol. 38, No. 12, 1998, pp. 1320-1325.
[8] V. Krebs, G. Furdin, J.F. Mareche, D. Dumay, "Effects of Coal Moisture Content on Carbon Deposition in Coke Ovens", *Fuel*, Vol. 75, No. 8, 1996, pp. 979-986.
[9] T. Nakagawa, T. Kudo, Y. Kamada, T. Suzuki, Y.Suzuki, I. Komaki, "Control of Carbon Deposition in the Free Space of Coke Oven Chamber by Injecting Atomized Water", *ISIJ*, Vol. 68, No. 7, 2002, pp. 386-392.
[10] V. Zymla, F. Honnart, "Coke Oven Carbon Deposits Growth and Their Burning Off ", *ISIJ*, Vol. 47, No. 10, 2007, pp. 1422-1431.
[11] C. Z. Lu, Y. P. Cao, "Study on Properties of Carbon Deposite in Coking Chamber and its Reaction Kinetics with Air", *Fuel & Chemical Processes*, Vol. 41, No. 1, 2010, pp. 15-18.
[12] S. R. Turns, *An Introduction of Combustion Concepts and Applications*, 3rd Ed., McGraw Hill, 2012.
[13] H. S. Caram, N. R. Amundson, "Diffusion and Reaction in a Stagnant Boundary Layer about a Carbon Particle", *Ind. Eng. Chem., Fundam.*, Vol. 16, No. 2, 1977, pp. 171-181.
[14] G. Adomeit, W. Hocks, K. Henriksen, "Combustion of a Carbon Surface in a Stagnation Point Flow Field", *Combustion and Flame*, Vol. 59, 1985, pp. 273-288.
[15] F. Yi, J.Fan, D. Ki, S. Lu, K. Luo, "Three-dimensional Time-dependent Numerical Simulation of a Quiescent Carbon Combustion in Air", *Fuel*, Vol. 90, 2012, pp. 1522-1528.

[16] P. A. Nikrityuk, M. Grabner, P. Kestel, B. Meyer, "Numerical Study of the Influence of Heterogeneous Kinetics on the Carbon Consumption by Oxidation of a Single Coal Particle", *Fuel*, Vol. 114, 2013, pp. 88-98.

[17] L. X. Zhou., *Combustion Theory and Chemical Fluid Dynamics*, Science Press, Moscos, 1986.

[18] B. F. Magnussen, B. H Hjertager, "On Mathematical Modeling of Turbulent Combustion with Special Emphasis on Soot Formation and Combustion" *Symposium (Int.) on Combustion*, Vol. 16, 1977, pp. 719-729.

[19] T. H. Shih, W. W. Liou, A. Shabbir, Z. Yang, J. Zhu, "A New k-ε Eddy-viscosity Model for High reynolds Number Turbulent Flows – Model Development and Validation," *Computer Fluids*, vol. 23, 2012, pp. 227-238.

[20] K. K. Kuo, *Principle of combustion*. New York: John Wiley and Sons, 1986.

[21] P. Cheng, "Two-dimensional radiating gas flow by a moment method," *AIAA Journal*, vol. 2, 1964, pp. 1662-1664.

[22] T. F. Smith, Z. F. Shen, and J. N. Friedman, "Evaluation of coefficients for the weighted sum of gray gases model," *J. Heat Transfer*, vol. 104, 1982, pp. 602-608.